Available online at www.sciencedirect.com

ScienceDirect

Energy Procedia 57 (2014) 662 – 671

Energy Procedia

2013 ISES Solar World Congress

Test and analysis of a flat plate latent heat storage design

M. Johnson*, M. Fiss, T. Klemm, M. Eck

German Aerospace Center (DLR), Pfaffenwaldring 38-40, 70597 Stuttgart, Germany

Abstract

Thermal storage technologies are a key component for increasing energy efficiency and assisting in the integration of regenerative energy sources in the energy market. In latent heat energy storage, the storage material changes phase as energy is charged into the storage. This makes use of the large amount of enthalpy that is absorbed or released during phase change of a material. Since a storage unit is a link in the chain between supply and demand of heat, it has to be adapted for each particular application. The aspect that is most difficult to adapt is the required power level. The inherent heat transfer in phase change materials (PCMs) is typically low and a limiting factor. Therefore, heat transfer structures have been developed that increase the surface area between the PCM and the heat transfer fluid. In proven design concepts for latent heat storage, a tube bundle is immersed in PCM as a heat exchanger between the storage medium and the heat transfer fluid. In order to increase the power level, the heat transfer surface is increased with exterior fins on the tubes.

A new concept that was designed, tested and analyzed at DLR is a storage adaptation of a flat plate heat exchanger. The design tested replaces the secondary heat exchanger medium with isolated chambers of storage material. The primary heat transfer fluid flows through the one side of the flat plate thermal storage, transferring heat across the steel encasements to the storage medium. A flat plate lab storage unit was built to prove this design concept. The testing of this storage unit, including various temperature gradients, flow rates and the insertion of heat transfer structures, is reported in this paper.

Selection and/or peer-review under responsibility of ISES.

Keywords: thermal energy storage; phase change material (PCM); flat plate design

* Corresponding author. Tel.: +49 711 6862 344; fax: +49 711 6862 747.
E-mail address: maike.johnson@dlr.de

Selection and/or peer-review under responsibility of ISES.
doi:10.1016/j.egypro.2014.10.221

1. Introduction

Storage in general buffers a component, in this case thermal energy, for later use. The buffer can be used to make one system usable for a longer period of time, as in solar thermal power plants, or to connect two systems that supply and demand energy at different times, as is more common in process heat applications. Since a storage unit is a combining link in the chain between heat supply and demand, it has to be adapted for each particular application. The adaptations include the temperatures (selection of the phase change material), capacity (PCM volume), flow (heat transfer fluid side dimensioning) and the power level, which is a function of the overall heat transfer coefficient. Thermal energy storages are typically classified by their storage system, which can be sensible, latent or thermochemical. In sensible storage, the storage changes temperature as the enthalpy level in the medium changes. A commercially available example of sensible storage is two-tank molten salt storage. By comparison, in latent energy storage, the storage material is a phase change material (PCM), which changes phase from, for example, solid to liquid as energy is charged into the storage. This makes use of the enthalpy that is released or absorbed during the phase change of a storage material and results in a higher storage capacity per unit volume over a small temperature range than typically found in sensible storage materials. In the third category, thermochemical storage, the storage material undergoes a chemical reaction that stores or releases thermal energy. These types of storage systems are still in the basic research stage. This paper describes research on latent energy storage units.

1.1. Heat transfer in latent heat storage

The storage medium energy can be transferred from the heat transfer fluid (HTF) indirectly via a tube/wall or other storage material containment structure. Various designs have been researched [1], including a storage variation of a tube and shell heat exchanger and of a flat plate heat exchanger. In both of these design types, the HTF flows through one side of the heat exchanger; on the other side, the storage PCM absorbs or releases heat by conduction and, to some extent, convection.

The overall heat transfer resistance is a sum of all of the system resistance components. This includes the heat transfer through forced convection of the HTF flow and the thermal conductivities of the containment and storage materials. The thermal conductivity of PCMs is inherent to the material and is typically low and a limiting factor [2]. In the solid state, the PCM therefore acts almost as an insulator. During the discharge of stored heat, the storage material solidifies from the heat transfer surface outwards and is thus a barrier between the heat transfer fluid HTF and the PCM. Although the thermal conductivity in liquid PCM is often not higher, natural convection occurs in liquid PCM, so that a higher heat transfer rate occurs in the liquid phase. Since the boundary barrier is formed during discharging and not during charging, thermal discharge rates are typically discussed.

In order to increase the possible power level, the heat transfer surface area has been increased. Storage designs using a tube-and-shell concept have been tested, with extended fins as the heat transfer structure. Sheet, radial and axial fins design concepts have been proven in various storage test units ([2], [3], [4]). Other concepts for increasing the overall heat transfer coefficient have also been reported [2].

In a latent heat storage system, the storage medium changes phase. This phase change is typically solid↔liquid, as this is the most pragmatically storable and containable phase change [5]. During the phase transitions, the storage medium undergoes an isothermal stage, during which the latent energy is stored to or released from the system (Fig. 1). If the heat transfer fluid is a single phase fluid, the temperature gradients between the storage medium and the heat transfer fluid vary throughout the charging or discharging process (Fig. 1a). This results in a less efficient heat transfer. If the heat transfer fluid changes phase simultaneously with the storage medium, the temperature gradient can be nearly constant throughout operation (Fig. 1b). For this reason, latent heat storage is quite suitable for water↔steam systems on the HTF side of the storage, such as in power plant cycles. For heat exchange to occur there needs to be a temperature gradient. This means that the HTF temperature for discharging heat needs to be lower and for charging higher than the phase change temperature of the storage material (Fig. 1, red/upper lines for charging and blue/lower for discharging). In a water/steam process, this results in higher pressures in the charging system and lower pressures in the discharging systems. These differences must be considered in the system design.

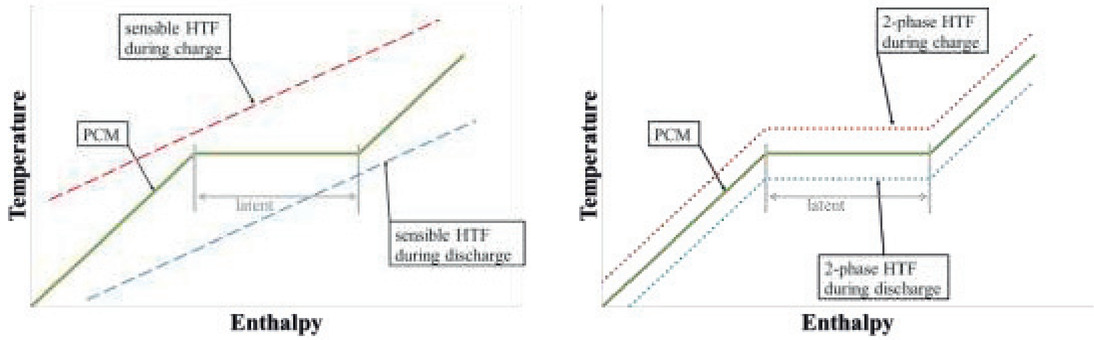

Fig. 1. Temperature-enthalpy diagrams for latent heat storage showing a (a) 1-phase and (b) 2-phase heat transfer fluid (adapted from [2] and [5]). Solid green line: PCM, charge/discharge; red/upper dashed (sensible) and dotted (2-phase) lines: HTF, charge; blue/lower dashed (sensible) and dotted (2-phase): HTF, discharge.

2. Novel flat plate heat storage

In this paper, the testing and simulation of a new flat plate heat storage unit is discussed. Flat plate heat storages have been studied for low temperature applications or with commercially available heat exchangers ([1], [6], [7]). Flat plate heat storages of a commercially available heat exchanger design were tested by Medrano using paraffin as the PCM [1]. As discussed in [1], a comparison of a compact heat exchanger to a commercially available flat plate heat exchanger of similar volume shows a much lower heat transfer area (factor of ~2.1) and a ~3.14 times smaller PCM volume for the flat plate heat exchanger. This shows an inefficient design ratio of material to total heat transfer.

2.1. Initial design

A flat plate heat storage unit was conceived [8] and designed specifically for energy storage – as opposed to commercially available heat exchangers, which are optimized for simultaneous heat transfer. The storage unit is an adaptation of the flat plate heat exchanger design in that the heat transfer fluid flows through headers into chambers between flat plates of steel, transferring heat through the steel plates to the PCM chambers. The HTF flows out through a second header back to the heat source/sink system. The heat storage design is shown in Fig. 2, schematically on the left (a) and as-built on the right (b).

In this design, the PCM chambers are open to the atmosphere and can be filled (and viewed) from above the storage unit. In addition, the design allows for a stress/strain-free volume change of the PCM during phase change. For this initial storage unit for testing, the unit is comprised of two outer, smaller PCM chambers to reduce environmental heat losses and two inner, wider PCM chambers for analysis. Between each of the PCM chambers is an oil chamber; all in all, there are three of these with the same approximate dimensions.

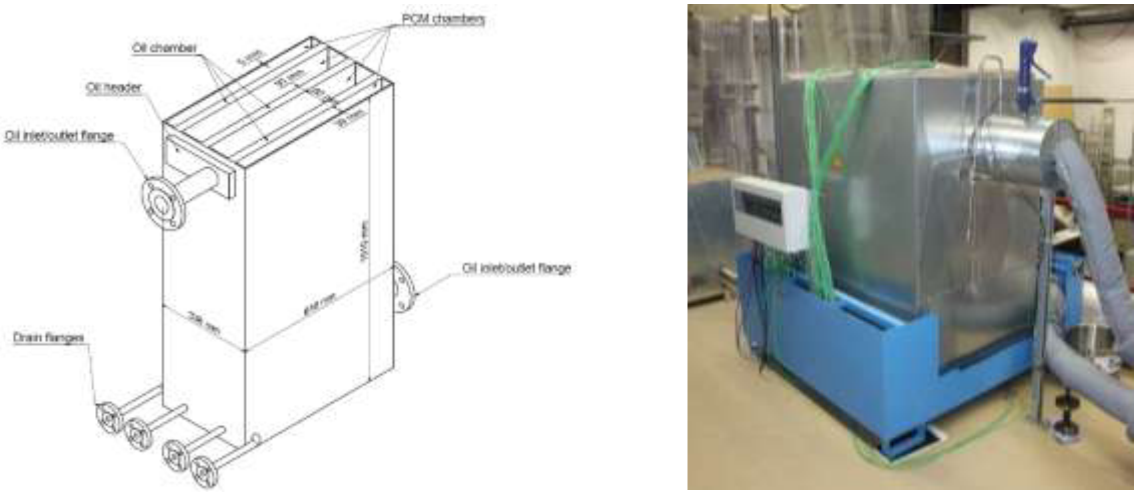

Fig. 2. (a) Drawing of the experimental latent heat storage unit. (b) Picture of assembled and insulated unit.

This storage unit is designed for operating temperatures up to 300 °C and is made of carbon steel 1.0425. In order to withstand the pressures in the HTF system, metal rods are welded to both the left and right sides of each HTF chamber. Each of the chambers is stiffened with 27 rods. The wider PCM chambers are about 8 cm wide. This very thick PCM layer was designed both to test the heat transfer in such a PCM block as well as to allow for modifications to the storage design, as discussed in section 2.2.

The properties of the PCM tested in this phase of the testing, a eutectic mixture of KNO_3-$NaNO_3$, as well as for other materials used in the storage unit and test loop, are shown in Table 1. The technical grade salt used in this storage had a melting temperature onset of 219.5 °C. This storage unit filled with this salt has a latent heat capacity of approximately 7.5 kWh.

Table 1. Material Properties for PCM [9], the HTF Mobiltherm 603, steel and aluminum.

Property/Material	Potassium nitrate – sodium nitrate (KNO_3-$NaNO_3$), eutectic	Mobiltherm 603	Steel 1.0425	Aluminum EN AW-5754
Ratio of KNO_3:$NaNO_3$	54:46 wt. %			
Thermal conductivity [W/(m·K)]	0.435 (at 222°C, liquid)	0.122 (at 200 °C)	51 (at 200 °C)	150 (at 20 °C)
Density, solid [kg/m³]	2050 (at 222°C)		7800 (at 20 °C)	2670 (at 20 °C)
Density, liquid [kg/m³]	1959 (at 222°C)	741 (at 200 °C)		
Specific heat [J/(kg·K)]	1350 (at 222°C, solid)/ 1492 (at 222°C, liquid)	2550 (at 200 °C)	540 (at 200 °C)	900 (at 20 °C)
Melting temperature [°C]	222 (pure) / 219.5 (technical grade)			
Latent heat [J/g]	108			

2.2. Design adaptations

The open chamber design of the flat plate storage allows for both a very simple initial filling of the storage as well as a simple adjustment of the storage heat rate by the addition of heat transfer structures. An adjustable design allows for a simple production of a basic storage unit that can be adapted to the application requirements with structures. Various structure geometries were considered and analyzed, both for their thermal efficiency as well as their feasibility. The displacement of PCM salt by the structure material was also considered. A good fin should theoretically transport heat easily to the middle of the PCM chamber while displacing a minimum amount of PCM. At the same time, it needs to be thermally cyclically stable, feasible to produce and allow for the volume change that occurs in PCM salts during phase change from solid to liquid. The structures analyzed were considered using the material aluminum, as this is readily available, has a high thermal conductivity (Table 1) and is thermally stable. Graphite sheets would also be feasible for some structure geometries. The designs analyzed are shown with some key parameters in Table 2.

Table 2. Analyzed heat transfer structures

Abbreviation	Descriptor	Drawing	Additional heat transfer surface area [m²]*	Structure volume [%]*	Phase change time during discharge [h]
None	None		0	0	5.51
WP	Waved profile		2.15	4.95	3.95
TP	Trapezoidal profile		2.15	4.96	3.69
RP	Rounded profile		2.27	5.21	4.63
ZZP	Zigzag profile		2.66	6.12	3.62
HP	Hollow profile		2.84	6.61	3.24
SCP	Semicircle profile	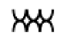	2.84	7.18	3.61
XP	X-profile		3.27	7.60	3.88
ZP	Z-profile		3.39	7.82	3.21
CP	Cross profile		3.75	8.66	2.64

* for comparison: using a 0.6 m x 0.93 m x 0.076 m chamber

The charge/discharge times of the geometry designs were simulated in a transient thermal model run with the method reported in [10]. This model takes latent heat and conductive heat transfer into account, but currently neglects convection. These times were calculated as comparative values using a temperature range of ±25 K and a convective heat transfer of the HTF of 200 W/(m²·K). Due to the large PCM pockets, especially in the storage with no heat structures, large discrepancies between simulated and experimental times are therefore expected. Based on the simulated times, the production feasibility and PCM displacement, the zigzag profile (design ZZP) was chosen for initial experimental testing.

3. Experimental testing

The goals of the experimental testing of the design concept were to prove the design concept with flat plate design and its adaptability. With the current design, a simple testing of design adaptability is possible, so that testing of changes in heat rate with various structures is possible. As the steels plates of the storage unit are not embossed as in commercially available flat plate heat exchangers, the fluid flow and therefore total heat transfer in the HTF chambers is optimized. The closed circuit pressure and rods for structural stability keep the fluid flow turbulent and therefore a good heat transfer was expected.

In order to understand the storage characteristics, the volumetric flow rate of the HTF and the temperature range about the melting temperature of the PCM were varied. A full parametric variation of the following two parameter variations was completed.

- Temperature range: ±10 K, ±18 K, ±25 K
- Volumetric flow rate: 0.5 m³/h, 2 m³/h

3.1. Test loop and data measurement

The storage unit was tested in a heating/cooling loop in the DLR lab facilities in Stuttgart, Germany. The loop uses the heat transfer fluid Mobiltherm 603 (properties shown in Table 1). The heating power is 12 kW and the cooling power is 30 kW. The maximum flow rate in the test loop is 3 m^3/h and the feasible temperature range is 20-300 °C. Through a valve bypass connection, it is possible to change the flow direction within the storage unit, so that the storage can be charged with one flow direction and discharged with the other. The storage unit is contained in a secondary oil container in case of leaks, and insulated on all sides. The insulation has a thickness of 25 cm and the thermal conductivity is rated at 0.05 W/(m·K). The test loop is controlled by a SPS unit from Siemens and data is stored at a 10 s interval.

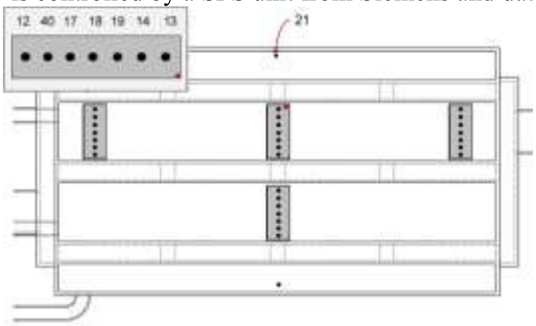

Fig. 3. Depiction of thermocouple placement in the storage unit. The thermocouples in the main chambers are held in place by steel plates, shown in grey.

Various data points are measured in the test loop. These include the temperature of the HTF at the inlet and outlet of the storage unit via Pt-100 resistance thermocouples, the differential pressure and volumetric flow rate in the HTF system, and the temperature in the PCM at various points via type K thermocouples. Calibration of the thermocouples showed a temperature difference of about 0.92 °C. This is within the error range of the thermocouples (minimum 1.5 °C) in this temperature range. The thermocouples for PCM temperature measurement were distributed over 3 measurement positions – left, middle and right – across the length of one of the middle PCM chambers (see Fig. 3). For comparison, the middle position was also measured in the second large PCM chamber. The thermocouples were positioned at half the height of the storage unit. At each of the left/right/middle positions, seven thermocouples were placed from front to back across the ca. 8 cm gap. The placement was affixed using a perforated sheet at the top of the storage for the length of the thermocouples and a metal plate near the ends of the thermocouples, which held them across the width of the storage at 1 cm intervals, as shown in Fig. 3 in grey. The goal of this placement is to measure the temperature distribution across both the width and length of the storage, in order to compare it to measurements with heat transfer structures and to overall gain an understanding of the heat transfer in the storage. In addition, a thermocouple was placed in each of the outer PCM chambers, one between the storage unit and the insulation and one on the outside of the insulation.

The temperature distribution of the HTF within the oil chambers can only be approximately measured by measuring the wall temperature on the PCM-chamber-side of the steel and calculating the approximate difference. In order to understand the flow in the oil chambers, thermocouples were clamped over the face of the steel plate to the oil chambers and the temperatures measured during heating and cooling of the oil in the HTF system prior to the PCM filling of the storage. These experiments showed a low temperature deviation from the left to right in the oil chambers (below 1 K) and the temperature deviation between the three oil chambers shown by differing average temperatures over time was between 1 to 1.5 K at 2 m^3/h.

Due to initial leaks from the HTF oil into the not-yet-filled PCM chambers, the storage unit had to be cut open and re-welded. This resulted in some irregularity in the width of the PCM chambers as well as an uneven steel wall. The unevenness in the wall due to the welds made an exact placement of some of the thermocouples in the PCM more difficult.

3.2. Comparison of results with and without heat transfer structures

3.2.1. Results and discussion, without heat transfer structures

As discussed above, a full parametric variation of the variables was tested. The discharging/charging cycle length was chosen to allow the storage unit to reach a steady state. The measurements during discharge of the storage unit without any heat transfer structures at a volumetric flow rate of 2 m³/h and a temperature range about the melting point of ±18 K is shown in Fig. 4. This temperature range corresponds to a charging temperature of 240 °C and a discharging temperature of 204 °C based on the theoretical melting temperature of the PCM. The red line for thermocouple 18 shows the temperature measurement in the middle of one of the large chambers (see Fig. 3 for thermocouple placement). This line shows a decrease in temperature from about 239 °C to about 220 °C.

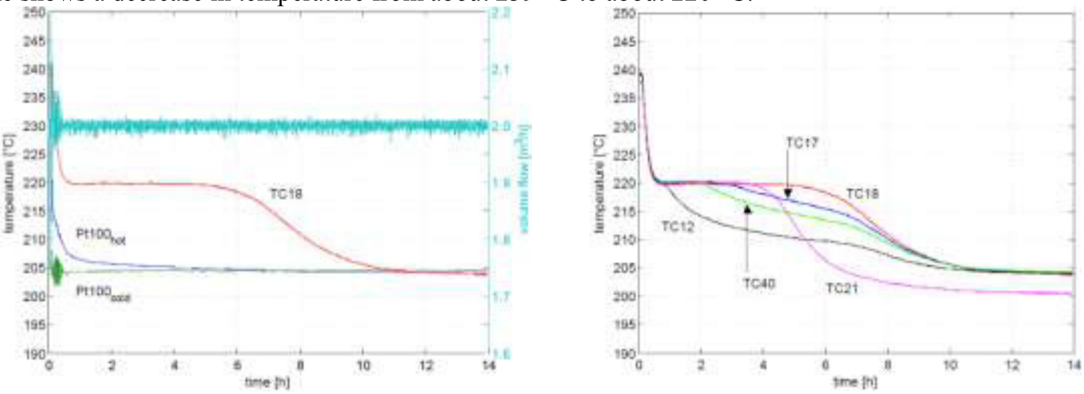

Fig. 4. Discharge, flow rate set to 2 m³/h, temperature range about the melting point ±18 K. (a) The line TC18 shows middle thermocouple measurement, $Pt100_{cold}$ the inlet oil temperature and $Pt100_{hot}$ the outlet oil temperature. (b) Thermocouple measurements in PCM, with TC12, TC40, TC17 and TC18 showing the temperature in the middle of the large chamber, with TC12 closest to the wall and TC18 in the middle of the chamber (see Fig. 3). TC21 is in one of the outer small storage unit chambers.

After the PCM temperature at TC18 reaches 220 °C after about 40 minutes, it plateaus into phase change for about 4 hours. After completing the phase change from liquid to solid, the salt then continues to drop in temperature through the release of sensible thermal energy until the discharge temperature has been reached. In Fig. 4a, the oil temperature at the inlet and outlet of the storage and the fluctuation of the volumetric flow are shown. Fig. 4b shows the thermocouple measurements from the same discharge run. Thermocouple 12 barely shows a phase change plateau, as it is very close to the heat source and steel wall. The other thermocouples successively have a longer phase change plateau. Thermocouple 21, in the outer and smaller chamber has a short plateau and also sinks to a lower discharge temperature. This thermocouple sees more environmental losses than the ones in the inner chambers.

Fig. 5 shows a comparison of the two different flow rates (a) and the three different temperature ranges (b) during discharging. On the left, the curve with a higher flow rate of 2 m³/h shows the same phase change time as the experiment with the slower flow rate of 0.5 m³/h, since the limiting factor for heat exchange remains the low thermal conductivity of the PCM. The sensible discharge post-phase change is

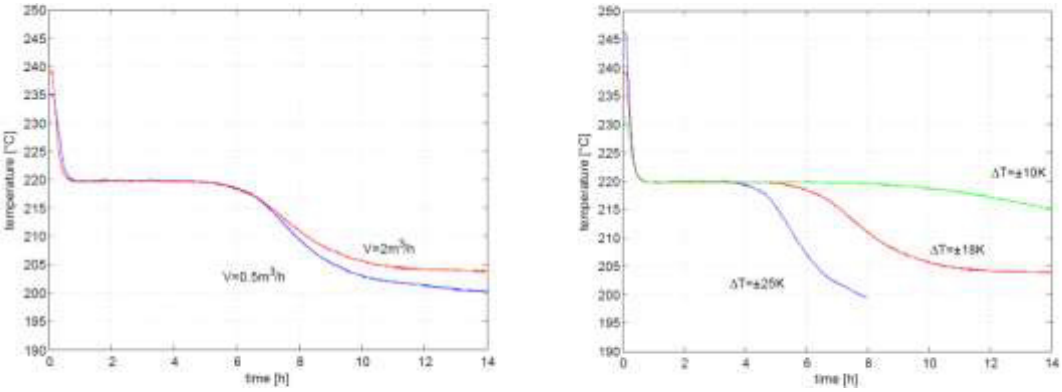

Fig. 5. Discharge, thermocouple TC18. (a) Discharge with a flow rate set at 2 m³/h and 0.5 m³/h, temperature range about the melting point ±18 K. (b) Discharge with a temperature range of ±10 K, ±18 K and ±25 K, flow rate at 2 m³/h.

somewhat faster at the slower flower rate and the starting and ending temperatures are lower. This is in general due to the higher environmental losses in the test loop before to the storage at the lower flow rate. In Fig. 5b, the temperature measurements of TC18 for the high/low temperature ranges of ±10 K, ±18 K and ±25 K about the melting temperature are shown for a flow rate of 2 m³/h. These show, as expected, a decreased phase change time with a higher temperature gradient. The time required for phase change for the middle thermocouple and therefore all of the PCM as well as total heat capacities are shown in Table 3. For compactness, the data for the experiments with the zigzag profile, discussed in 3.2.2, are shown here as well.

Table 3. Total heat discharged from the storage, calculated as well as measured for both flow rates, without a profile and with ZZP.

Temperature Range	Heat, theoretical [Wh]	None, Heat, 2 m³/h [Wh]	None, Heat 0.5 m³/h [Wh]	None, PCT*, 2 m³/h [h]	ZZP, Heat, 2 m³/h [Wh]	ZZP, Heat, 0.5 m³/h [Wh]	ZZP, PCT*, 2 m³/h [h]
+-25 K	12383	13291	12422	2.75	12969	NA**	1.55
+-18 K	11008	10447	9743	3.75	10470	NA**	1.85
+-10 K	9436	6569	6229	5.40	6864	6797	3.30

*PCT: Phase change time; **Test runs not completed at the time of paper submission.

The heat flow over the storage unit, shown in Fig. 6a, is a function of density, volumetric flow rate, specific heat and the difference between the inlet and outlet temperatures of the HTF. The properties for density and specific heat of the HTF were determined for the average of the inlet and outlet temperatures at each measurement time. The heat flow sinks below zero towards the end of discharging due to heat losses. There is a steep incline in heat flow during the sensible part of the discharge (the first ca. 40 min., see Fig. 5b), as heat is transferred quickly from the liquid PCM to the steel. Thereafter, the heat flow sinks steadily as the solidified PCM barrier-layers on the steel plates grow, thereby increasing the total thermal resistance to the not-yet-discharged liquid PCM in the middle. The theoretical heat, not regarding losses, that can be discharged at the three temperature ranges and the measured/calculated heat for both flow rates are shown in Table 3. The heat was summed until zero was reached, which is different for each of the data sets. Due to the longer experimental run time at smaller temperature ranges, the overall losses are greater here, thereby resulting in a larger discrepancy to the simulated values. The simulated time required for phase change at a temperature range of ± 25K (see Table 2) was 5.51 h, comparing to 2.75 h for the same temperature range experimentally, showing that the missing convective element and/or the estimated convective heat transfer from HTF to PCM are critical for determining an accurate time.

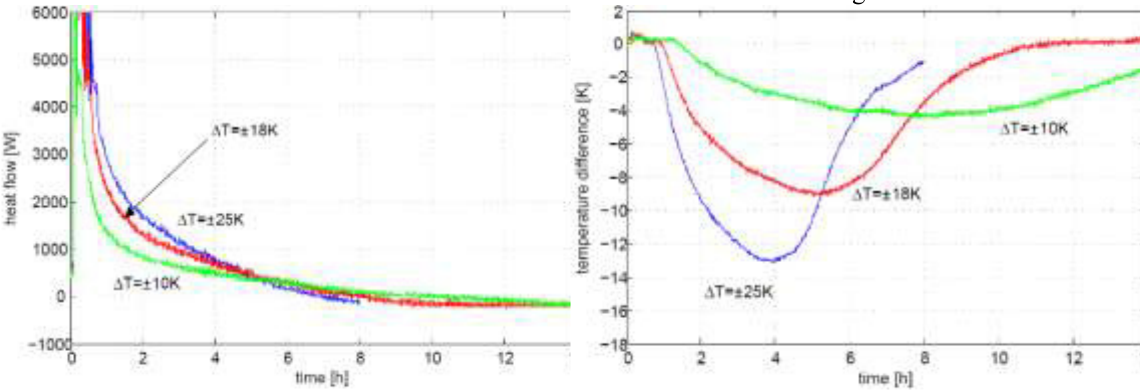

Fig. 6. Discharge, with the temperature ranges of ±10 K, ±18 K and ±25 K, flow rate at 2 m³/h. (a) Heat flow from the storage into the HTF. (b) Temperature difference between inner (TC18) and edge (average of TC12 and TC13) PCM temperatures.

Fig. 6b shows the temperature difference between the middle of the PCM chamber measured by TC18 and the edge of the PCM chamber over the distance between these two points. The edge temperature is an average of TC12 and TC13 (see Fig. 3). After parts of the PCM start phase change (for all three temperature ranges after about 40 minutes) the temperature difference increases, corresponding to the sinking temperature at the edge of the PCM chambers. The edge PCM has been discharged, but continues to conduct heat from inner PCM regions to the steel. Each of the curves reaches its nadir at the end of the phase change time for that experiment (compare Fig. 5). Thereafter, the temperature at the middle of the PCM also sinks slowly until the discharge temperature is reached.

3.2.2. Results and discussion, with zigzag heat transfer structure

As an adaptation, the zigzag structures were sunk into the PCM chambers. PCM was removed from the chambers so that each was at the same fill-level as without the profile. A comparison of a

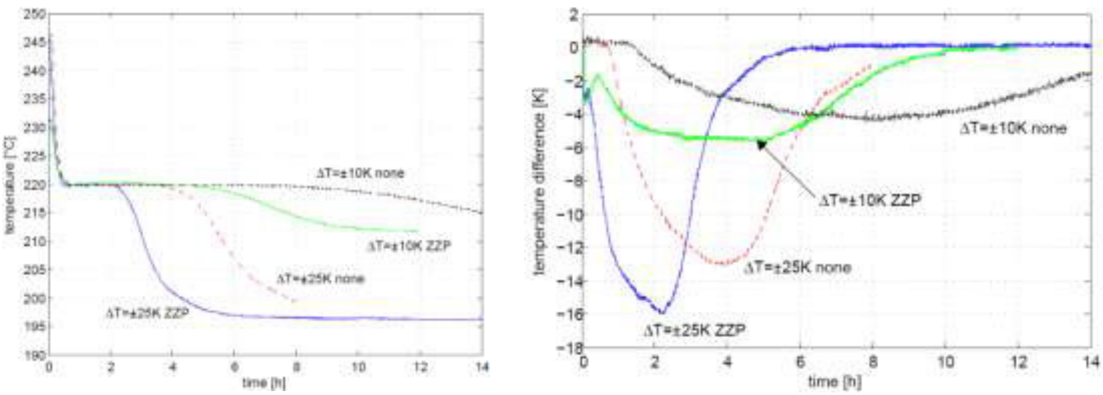

Fig. 7. Comparison of the ±10 K and ±25 K temperature ranges for experiments with the zigzag profile and without a profile with a 2 m³/h flow rate during charging showing (a) the temperature of TC18 and (b) temperature difference between inner (TC18) and edge (average of TC12 and TC13) PCM temperatures.

thermocouple measurement during discharge for the runs without structures and with the zigzag structures for two temperature ranges is shown in Fig. 7. The temperature profiles of the middle thermocouple show a significant decrease in the time needed for phase change to be completed. These are listed in Table 3.

The temperature difference between inner (TC18) and edge (average of TC12 and TC13) PCM temperatures in Figure 7b, which is proportional to the heat flux, shows a similar trend, with the nadirs of each of the runs with ZZP lower than without. Comparing the time to complete phase change of the ±25 K range without heat transfer structure of 2.75 h (see Table 3), it is possible to decrease the temperature needed to achieve a similar phase change time by using heat transfer structures (±10 K range with ZZP, 3.30 h). By keeping a constant temperature range and adding heat transfer structures, a decrease in phase change time from 2.75 h to 1.55 h while increasing the heat rate is possible.

4. Conclusions and further testing

The first results of a novel flat-plate phase change heat storage unit are presented. The unit was tested experimentally, without and with heat transfer structures to adjust the heat flow rate. First results prove the functionality of the design in both configurations. Addition of the heat transfer structures improves the performance of the storage unit noticeably, as expected. With this flexibility, the same heat storage was able to provide phase change discharge times of between 2 and 8 hours, making it adaptable for a wide range of applications. Through further adjustment of the phase change chamber gap (currently 8 cm) and the heat transfer structures, further heat rate adjustments are possible. Through an optimization of the heat transfer plates, currently made of sheet metal, the heat transfer from the HTF can be further improved and the storage unit more efficiently designed. Further testing will include investigations with other heat transfer structures, such as trapezoidal profiles, as well as a comparison with simulation results for further design adaptations.

References

[1] Medrano M, Yilmaz MO, Nogués M, Martorell I, Roca J, Cabeza LF. Experimental evaluation of commercial heat exchangers for use as PCM thermal storage systems. Applied Energy 86 (2009),2047-55, doi:10.1016/j.apenergy.2009.01.014.

[2] Tamme R, Bauer T, Buschle J, Laing D, Mueller-Steinhagen H, Steinmann W-D. Latent heat storage above 120 °C for applications in the industrial process heat sector and solar power generation. Journal of Energy Research 2008, 032736017(July 2007), 264-271, doi:10.1002/er.

[3] Laing D, Bauer T, Breidenbach N, Hachmann B, Johnson M. Development of high temperature phase-change-material storages. Journal of Applied Energy 2012; http://dx.doi.org/10.1016/j.apenergy.2012.11.063, 2013.

[4] Laing D, Bahl C, Eickhoff M, Fiss M, Hempel M, Meyer-Grünefeldt M. Test Results of a Combined Storage System for Parabolic Trough Power Plants with Direct Steam Generation. ASME 5th International Conference on Energy Sustainability 2011.

[5] Mehling H, Cabeza L F. Heat and cold storage with PCM. Berlin: Springer Verlag; 2008.

[6] Amin N a M, Belusko M, Bruno F, Liu M. Optimising PCM thermal storage systems for maximum energy storage effectiveness. *Solar Energy* (2012), *86*(9), 2263-72. Elsevier Ltd. doi:10.1016/j.solener.2012.04.020.

[7] Liu M, Bruno F, Saman W. Thermal performance analysis of a flat slab phase change thermal storage unit with liquid-based heat transfer fluid for cooling applications. *Solar Energy*, 2011, *85*(11), 3017-3027. Elsevier Ltd. doi:10.1016/j.solener.2011.08.041.

[8] Fiss M, Wärmespeichervorrichtung, Deutsches Patent- und Markenamt, DE 10 2011 001 883 A1 2012.10.11, filed April 7, 2011 and disclosed October 11, 2012.

[9] Bauer T, Laing D, Tamme R. Overview of PCMs for concentrated solar power in the temperature range 200 to 350°C. Advances in Science and Technology Vol. 74 (2010) 272-7, doi:10.4028/www.scientific.net/AST.74.272.

[10] Johnson M, Breidenbach N, Laing D, Hachmann B. Experimental and numerical analysis of a phase change storage. Solar 2013. Baltimore, MD, USA, 2013.